International Journal of
Oral and Dental Health

Perchyonok et al. Int J Oral Dent Health 2015, 1:3
ISSN: 2469-5734

Research Article: Open Access

Hydroxyapatite/Nanodiamond Hydrogels as Potential Materials for Temporomandibular Joint Disfunction: from Design to Performance *in vitro*

V. Tamara Perchyonok[1,2]*, Shengmiao Zhang[3], Tatiana Souza[1], Nickolas Basson[4], Desigar Moodley[4] and Sias Grobler[4]

[1]*VTPCHEM PTY LTD, Glenhuntly, Victoria, Australia*

[2]*Health Innovations Research Institute, RMIT University, Melbourne Australia*

[3]*School of Material Science and Engineering, East China University of Science and Technology, China*

[4]*Oral and Dental Research Institute, School of Dentistry, The University of Western Cape, Cape Town, South Africa*

***Corresponding author:** *V. Tamara Perchyonok, Health Innovations Research Institute, RMIT University, Melbourne Australia, E-mail: tamaraperchyonok@gmail.com*

Abstract

The aim of this investigation is to evaluate the suitability and flexibility of the designer materials consisting of chitosan, nanodiamond, hydroxyapatite and therapeutic agent such as tetracycline and potential antioxidant such as B12 to act as an "*in vitro*" probe to gain insights into molecular origin of TMJ and apply the newly developed materials for the evaluation of new therapeutic treatment modalities in the TMJ therapy *in vitro*. Mechanical properties of new materials, such as tensile strength, compressive strength and modulus of elasticity were measured as well as drug release of tetracycline assessed. The results of this study demonstrate the potential of using HA/Nanodiamond chitosan hydrogels as bioactive cements and *in vitro* probes for the detection of free radical damage associated with TMJ and other relevant free radical generated conditions. The added benefits of the chitosan/nanodiamond/hydroxyapatite treated hydrogels involved positive influence on the tetracycline release, sustainable bio-adhesion, tensile strength, compressive strength as well as modulus of elasticity of the hydroxyapatite containing materials in the "*in vitro*" systems was tested and demonstrated *in vitro* "build in" free radical defense mechanism.

Keywords

Hydroxyapatite, Drug release, Nano-diamonds, Mechanical Properties

Introduction

In the last few decades, tissue engineering has emerged as a promising multidisciplinary approach for the repair and regeneration of damaged bone tissue [1-3]. The craniofacial structure consists of bone, cartilage, soft tissue, nerves, and blood vessels [4]. The major materials used in craniofacial tissue engineering are natural and synthetic polymers, ceramics, composite materials, and electrospun nanofibers [5].

Biomaterial to be used as a scaffold must possess sufficient mechanical strength, large pore volumes and pore interconnectivity to allow continuous tissue in growth, and transport properties to allow the influx of nutrients and elimination of waste products [6]. Randomly positioned pores contribute to better cell seeding and better cell aggregation in the designed scaffolds [7]. Natural scaffolds like collagen type I, chitosan, calcium alginate, hyaluronic acid, and composites have been shown to be osteo-conductive, but with problems like lack of mechanical strength when implanted, risk of infection, immunogenicity, and rapid degradation rate [8,9].

Scaffolds are the mechanical constructs that act as carriers for cells and/or growth factors. The main role of scaffolds is to simulate the extracellular matrix for cell adhesion, migration, proliferation, and differentiation [10,11]. The molecular events that underline the degenerative temporomandibular joint (TMJ) diseases are poorly understood [12]. Mechanical stresses are generated during functional or para-functional movements of the jaw; adaptive mechanism of the TMJ may be exceeded by free radical accumulation leading to a dysfunctional state (i.e. disease state) [13].

Specific bacterial organisms such as *Staphylococcus aureus, Streptococcus mitis, M. fermentas, Actinobacillus acinomycetemcomitans* have been found in the synovial fluid of TMJ/TMD affected patients. Serum antibodies against Chlamydia species in patients with mono arthritis of the TMJ have also been reported [14].

Chitosan (CS), obtained through the alkaline deacetylation of chitin, is a copolymer of N-acetyl-D-glucosamine and D-glucosamine. CS stands out by a unique combination of favorable biological properties such as nontoxicity, biocompatibility and biodegradability, along with mucoadhesive, bacteriostatic, and wound-healing properties [15-17].

ClinMed International Library

Citation: Perchyonok VT, Zhang S, Souza T, Basson N, Moodley D, et al. (2015) Hydroxyapatite/Nanodiamond Hydrogels as Potential Materials for Temporomandibular Joint Disfunction: from Design to Performance *in vitro*. Int J Oral Dent Health 1:015

Received: August 01, 2015: **Accepted:** September 09, 2015: **Published:** September 12, 2015

The aim of this investigation is to evaluate the suitability and flexibility of the designer materials consisting of chitosan, nanodiamond, hydroxyapatite and therapeutic agent such as tetracycline and potential antioxidant such as B12 to act as an "*in vitro*" probe to gain insights into molecular origin of TMJ and apply the newly developed materials for the evaluation of new therapeutic treatment modalities in the TMJ therapy *in vitro*.

Methods

Preparation of various hydrogels: general protocol

The therapeutic agent containing gel was prepared by dispersion of 0.2 gm in glycerol (5% w/w) (1 ml) using a mortar and a pestle following the earlier reported generic protocol [15-17]. Ten milliliters of glacial acetic acid (1% w/w) was then added with continuous mixing and finally chitosan: hydroxyapatite: nanodiamond (1:1:1 mixture w/w chitosan: hydroxyapatite: nanodiamond powder) polymer was spread on the surface of the dispersion and mixed well to form the required gel [18]. The strength of the prepared gel (10 gm) is 0.2 g of active ingredient by weight in each gram of the base.

Morphology of the gels

The samples were prepared by freezing in liquid nitrogen for 10 min, and then were freeze-dried for 24 h [15-18]. The prepared samples were fractured in liquid nitrogen using a razor blade. The fractured samples were attached to metal stubs, and sputter coated with gold under vacuum for SEM. The interior and the surface morphology were observed in scanning electron microscope (SEM, Hitachi S4800, Japan).

Gel stability

Stability of the gel formulations was also investigated. The organoleptic properties (color, odor), pH, drug content, and release profiles of the gels stored at 20°C were examined on days (0, 15, 30 and 178) [15-18].

Tetracycline release and biomaterials

The release study was carried out with USP dissolution apparatus type 1, Copley U.K., slightly modified in order to overcome the small volume of the dissolution medium, by using 100 ml beakers instead of the jars. The basket of the dissolution apparatus (2.5 cm in diameter) was filled with 1 gm of tetracycline gel on a filter paper. The basket was immersed to about 1 cm of its surface in 50 ml of phosphate buffer pH 6.8, at 37°C ± 0.5 and stirred at 100 rpm. 24 Samples (2 ml) were collected at 0.2, 1, 2, 3, 4, 5, 6, 7, 8, 10, 15 and 24 hours and were analyzed spectrophotometrically with a U.V. spectrophotometer (Cintra 5, GBC Scientific equipment, Australia). The UV-vis absorption spectrum of tetracycline hydrochloride in water is typical at 361 nm, using the calibration curves ($A^{1\%}_{1cm}$ = 337 for tetracycline hydrochloride both evaluated in PB, pH 6.8). Three replicate measurements were performed for each designed formulation [19,20]. Each sample was replaced by the same volume of phosphate buffer pH 6.8 to maintain its constant volume and sink condition [20,21].

Bio-adhesive investigation

Bio-adhesion studies were done using a Chatillon apparatus for force measurement [22]. This method determines the maximum force and work needed to separate two surfaces in intimate contact [23]. The hydrogels (0.1 g) were homogeneously spread on a 1 cm^2 glass disk and then the disks were fixed to the support of the tensile strength tester using double sided adhesive. The gel was brought into contact with a slice of dentin was established in order to imitate adhesion of the gel to the "hydroxyl-apatite prototype system" structure. After a preset contact time of 1 min under a contact strength of 0.5 N, the 2 surfaces were separated at a constant rate of displacement of 1 mm/s. The strength was recorded as a function of the displacement, which allowed to determine the maximal detachment force, F_{max}, and the work of adhesion, W, which was calculated from the area under the strength-displacement curve [23].

Protein cross-linking as a model for detection of free radical activity and activation of "molecular defense forces"

Bovine serum albumin (BSA), a completely water-soluble protein, was polymerized by hydroxyl radicals generated by the Fenton reaction system of Fe^{2+}/EDTA/ H_2O_2/ascorbate [15-18]. As a result, the protein loses its water-solubility and the polymerized product precipitates. The decrease in the concentration of the water-soluble protein can easily be detected.

The *in vitro* incubation mixtures contained reagents, added in the sequence as follows, at the final concentrations: bovine serum albumin (0.8 mg/ml), phosphate buffer, pH 7.4 (10 mM), water to reach 2.5 ml total volume, antioxidant (such as B12, N-acetyl cysteine and corresponding chitosan/hydroxyapaitite hydrogels) tested to reach required concentration as shown in results, EDTA (0-/4.8 mM), $Fe(NH_4)_2(SO_4)_2$ (0-/4 mM), ascorbate (4 mM) and H_2O_2 (0.2%). To chelate iron completely, 1.2 molar excess of EDTA was always use [21]. The reaction mixture was incubated for 20 min at ambient temperature. The supernatant was precipitated with an equal volume of trichloroacetic acid (10%) at 0 degrees Celsius. The precipitate thus obtained was re-dissolved in 1 ml of Na_2CO_3 (10%) in NaOH (0.5 M) and the final volume made up to 2.5 ml by water. An aliquot of the solution was used for protein determination [24]. The yield of OH radicals generated in the incubations was determined on the basis of degradation of deoxyribose [25]. Bityrosine formation was monitored by measuring fluorescence at 325 nm (excitation) and 415 nm (emission) according spectrophotometer [26].

Swelling/weight loss tests and bioactive release

The swelling/weight loss tests were performed when triplicates of each samples composition (approximately 2 cm^2, weight normalized) were immersed in 2 mL of different fluids at 37°C for each time interval studied (1, 2, 4, 24, and 96 h). Two different media were used in accordance with the ISO 10993-9 standard. The first media was Phosphate Buffered Saline (PBS, Sigma Aldrich), intended to mimic the inorganic phase of human plasma [27]. The other media was PBS with a reduced pH which was intended to simulate the local inflammatory environment of the wounds [28,29]. This is termed Solution pH 4.0. The pH was lowered using Lactic Acid (Sigma Aldrich). The fluid absorption of each sample was calculated according to equation to obtain their swelling degree (SD) (Equation 1). WS is the weight of the sample at each time interval (swollen weight) and WD is the dry weight before swelling [30]. After 4 days of immersion, the samples were dried and weighed in order to calculate their weight loss (WL) [eq. 2, where W_D and W_{DS} are the weight of the dried samples before and after swelling tests, respectively.

Equation 1: $SD = 100\ (W_S\text{-}W_D)/W_D\ (\%)$

Equation 2: $WL = 100\ (W_D - W_{DS})/W_D\ (\%)$

Equations 1: Equation to calculate a swelling degree (SD) and **Equation 2**: Equation to calculate weight loss.

Mechanical characterization of the new materials

Tensile strength: Tensile testing was conducted using Instron 5565. Following American Standardized Testing Materials Standard D3039, rectangular samples were approximately 6-8 mm in length, 1mm in width of 1 mm in thickness, and tested with a gauge length of 3.5 ± 0.4 mm [30]. Samples were elongated at a rate of 1% of gauge length per second. The cross-sectional area of samples was evaluated using ImageJ image analysis software. Stress-strain curve were developed from the load-displacement curve. Young's modulus was quantified by finding the slope of the stress strain curve, and ultimate tensile strength was calculated [30].

Compressive strength and elastic modulus: The hydrogels with dimensions of 10 × 10 × 5 mm^3 were used for a compression test using Instron by applying load via 1N load cell at a crosshead speed of 2 mm/min in ambient conditions [30]. The stress-strain curve obtained was used to determine mechanical properties. The compressive strength and elastic modulus was determined from the maximum

load recorded and from the slope at the initial stage (< 2% strain), respectively. Five specimens were tested for each condition.

Biodegradation: The hydrogels containing hydroxyapatite additives and having similar weight and dimensions of approximately 0.8-1.0 g and 20 × 20 × 6 mm^3, respectively, were immersed into a glass bottle containing 100 ml phosphate buffer saline (PBS; Sigma-Aldrich, Australia) medium under 37°C at pH 7.4 for a period up to 7 days. At predetermined periods of time, the samples were taken out and vacuum dried for 24 hours. The dried samples were weighted to determine the biodegradation rate.

Microbiology investigations: A type strain of *Staphylococcus aureus* (ATCC 12600), obtained from the American Type Culture Collection (Manassas, USA) was used as test bacterium for estimating the antibacterial activity of the hydrogels. The antibacterial activity of the prepared chitosan hydrogels were tested using the standard Kirby-Bauer agar disc diffusion method [31,32]. Five to 6 mm deep Muller-Hinton agar (Oxoid, Basingstoke, UK) plates were inoculated by streaking a standardized inoculum suspension that match a 0.5 McFarland standard and containing 10^7-10^8 colony forming units/ml with a throat cotton swab. For each test sample 500 µg of hydrogel was applied to a 6 mm diameter paper disc. The paper discs were placed on the inoculated Muller-Hinton agar medium and incubated at 37°C for 24 hours. The diameter of the zones of growth inhibition was measured with a caliper. Each measurement was done in triplicate and the testing of each sample was repeated 3 times. The antibacterial efficacy of the prepared gels were compared to antibiotic sensitivity discs (Mast Laboratories, Merseyside UL) containing 30 µg of tetracycline per disc.

Results

Modified antibiotics hydrogels

The SEM images were obtained to characterize the microstructure of the freeze-dried gels and are presented in figure 1. The 'skin' of the prepared modified flowable composites can be seen, and the collapse of the surface pores may be due to artifacts (freeze-drying process).

Swelling and bio-additive release for the newly prepared hydrogels

The swelling tests in PBS and in Solution pH 4.0 for 4 days revealed that when reaching the equilibrium swelling degree (ESD), all samples swelled in accordance with (Figure 2a and Figure 2b). Based on the ESD values, the gels can be considered as superabsorbent [33]. A peak of media uptake was observed at the beginning of all curves, and after 1 day of swelling there was a plateau-the ESD. The ESD occurs when the hydration forces (the network stretching by the initial fluid uptake) and the elastic force of the cross-linkages reach the equilibrium [34,35]. It is well documented that, high amounts of bioactive led to low degree of crystalinity and low percentage of crystalline phase. When the samples swell, the amorphous chains could have more freedom to move and, if they were not cross-linked, with the help of the media, they could detach from the network to the media, increasing the weight loss [36].

The swelling tests in PBS and in Solution pH 4.0 for 4 days revealed that when reaching the equilibrium swelling degree, all samples swelled in accordance with (Figure 2a and Figure 2b). Based on the cumulative swelling values, the gels can be considered as superabsorbent [33]. A peak of media uptake was observed at the beginning of all curves, and after 1 day of swelling there was a plateau.

In vitro release of antibiotics

Drug release from topical formulations is affecting the efficiency of topical therapies to a great extent. Tetracycline, a model antimicrobial drug, which can be used in topical wound treatment, was incorporated into chitosan/hydroxyapatite/nanodiamond-based delivery systems and cumulative release was tested and results are summarized in figures 3a and figure 3b respectively [34]. After a 4 day time period, no significant difference in drug release could be seen between the different formulations of functionalized materials.

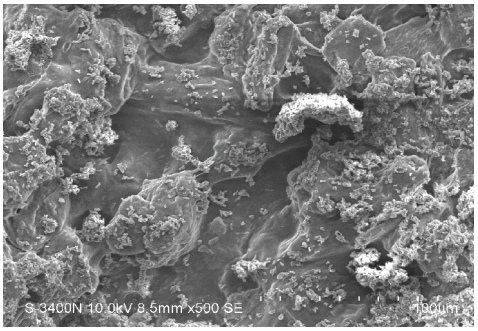

a. NanoChTetr

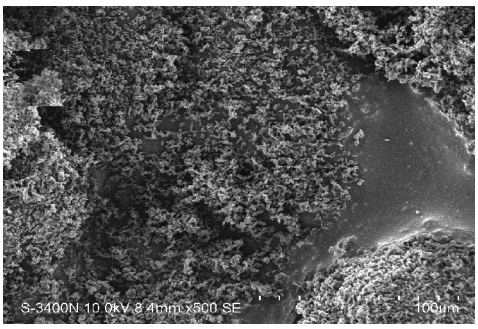

b. NanoTetr

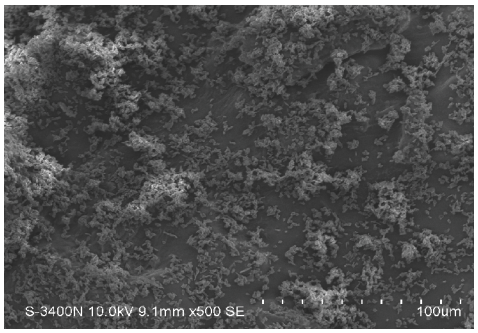

c. NanoHatetr

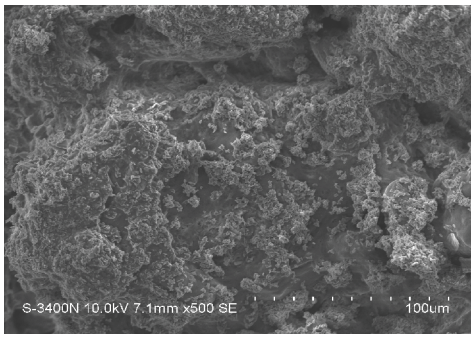

d. Nanochtetrha

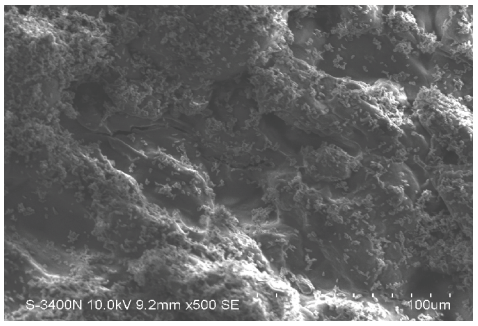

e. NanoChTetrHaB12

Figure 1: SEM of the surfaces of the materials after polymerization where a. NanoChTetr, b. NanoTetr, c. NanoHatetr, d. Nanochtetrha and e. NanoChTetrHaB12.

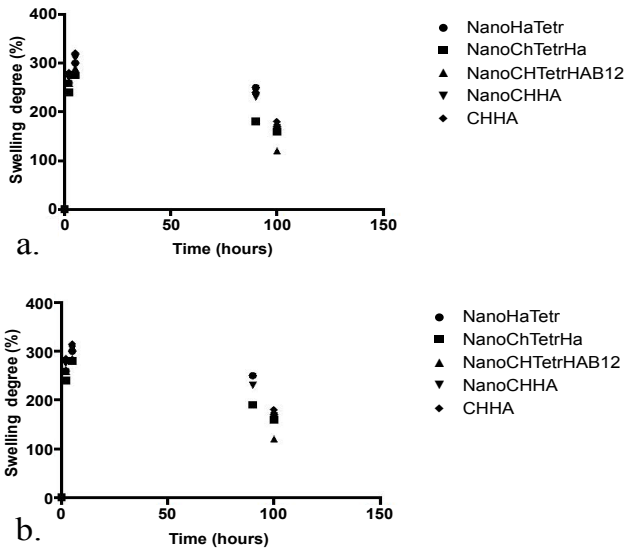

Figure 2: Swelling degree (SD) results of Ch/HA and of Ch/HA–nanodiamond/ therapeutic agent samples, after regular time intervals (1, 2, 4, 24, 96 h), when immersed in (a) PBS and (b) Solution pH 4.0 for 4 days.

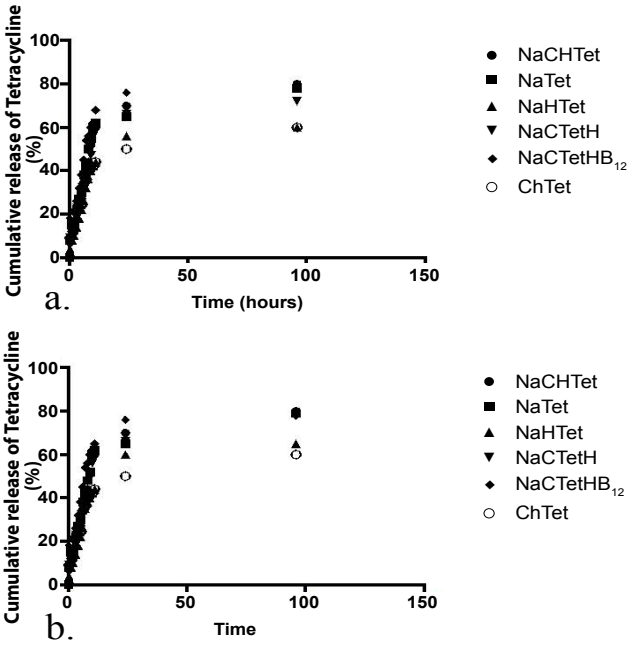

Figure 3: Tetracycline cumulative release profile of Ch/HA/Nanodiamond–tetracycline samples. The Ch/HA/ Nanodiamond tetracycline samples were immersed in (a) PBS and (b) Solution pH 4.0 and the propolis delivered was quantified after regular intervals of time for 4 days.

Tetracycline release is expected to be fully diffusion controlled as the cumulative percentage of drug released is proportional to the square-root of time. The regression lines show a good fit with $R^2 \geq 0.97$. Higuchi reported this kind of relation between release and square-root of time for suspension-ointments originally [35].

Bioadhesion and CH/Nano/HA hydrogels

Higher adhesiveness of the gels is desired to maintain an intimate contact with condyle of the mandible and the mandibular fossa in the case of articular disc of the TMJ joint, therefor bio-adhesion between the newly prepared hydrogel (CH/Nano/HA hydrogels) was tested against tooth structure and results are summarized in table 1. Chitosan hydrogels showed the highest adhesive force and the work of adhesion this can be expected because of the well-known intrinsic bioadhesive properties of chitosan [36]. The adequate water absorption capacity together with the cationic nature which promotes

Table 1: Bioadhesion testing *in vitro*.

Hydrogel	Adhesive Force (N) ± SD (Dentin)	Work of Adhesion (Ncm) ± SD (Dentin)
NanoCHTetr	1.09 ± 0.35	3.12 ± 0.38
NanoCHTetrHA	1.21 ± 0.47	3.49 ± 0.42
NanoCHTetrHAB12	1.08 ± 0.40	3.14 ± 0.29
CH/HA	0.98 ± 0.24	2.92 ± 0.34

The presented values are an average (n = 5)

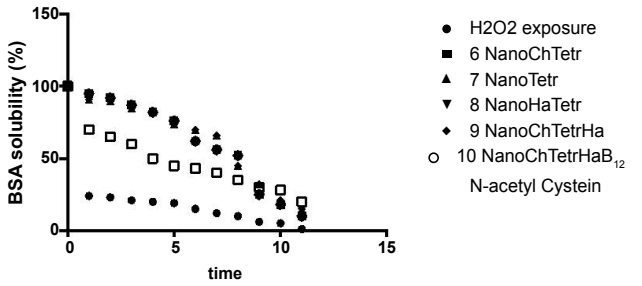

Figure 4: Free radical defense and biomaterials as a function of the BSA solubility (%) at pH 6.7.

binding to the negative surface of skin or dentin structure can also interpret this results.

Chitosan hydrogels showed the highest adhesive force and the work of adhesion this can be expected because of the well-known intrinsic bioadhesive properties of chitosan. The adequate water absorption capacity together with the cationic nature, which promotes binding to the negative surface of skin or dentin structure can also interpret this results. According to Caffaggi, hydration of the polymer causes mobilization of the polymer chains and hence influences polymeric adhesion [37]. Appropriate swelling is important to guarantee adhesivity; however, over hydration can form slippery non-adhesive hydrogels [38]. In addition the molecular arrangement of the polymeric chains, which are present in the new hydrogels, such as propolis, aspirin, ibuprofen and naproxen can further unable to interact further with the substrate the correlation between the force and work of adhesion is noticeable for all.

NDs, as a new member of carbon nanoparticles family, have emerged as an alternative promising material for building drug delivery systems with high efficiency and low toxicity owing to their superior physico-chemical properties and good biocompatibility [39]. Currently, NDs are used as a drug carrier mainly in two forms: (1) NDs assemble on a chemical substrate to form a thin film, having interactions with a drug in two-dimension; (2) NDs form spontaneous clusters also named as ND hydrogel with low free energy in an aqueous solution, having interactions with a drug in three-dimension [40]. The detailed investigation of the newly produced hydrogels with particular attention being paid towards understanding of the exact nature of interaction between nano-diamond, chitosan and hydroxyapatite are currently on the way in our laboratory.

Bioactivity of hydrogels and free radical defense in the TMJ model *in vitro*

Inflammation of the temporomandibular joint (TMJ) is often treated with arthrocentesis, which is thought to have an anti-inflammatory effect [41]. In this study, we focused on developing an *in vitro* bio-functional model of initiating a free radical formation such as exposing peroxide under Fenton conditions and monitoring the free radical defense capacity of the nanodiamond: chitosan hydrogels as a measure of extend the water solubility of BSA (Bovine Serum Albumin) protein as demonstrated in figure 4. The main biochemical principle behind this reliable and easily adjusted model is that in the presence of iron Fe^{2+} and H_2O_2, hydroxyl radicals are released that cause oxidative stress in living systems [42].

Mechanical properties of newly prepared materials

The articular surfaces in general and articular disc in particular

Table 2: Mechanical properties (such as compressive strength and Elastic modulus) of hydrogels without and with HA additive.

Mechanical properties	Pure HA	NanoHaTetr	NanoChTetrHa	NanoCHTetrHAB12
Compressive strength(MPa)	0.16 ± 0.04	0.26 ± 0.06	0.28 ± 0.05	0.35 ± 0.07
Elastic modulus (MPa)	0.79 ± 0.04	1.00 ± 0.16	1.12 ± 0.25	1.32 ± 0.27

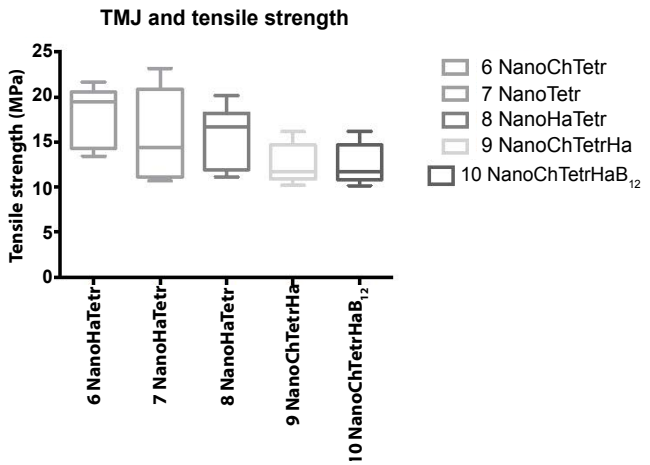

Figure 5: Tensile strength of the modified biomaterials.

are highly incompatible. Due to this incompatibility, the contact area of the opposing articular surfaces are very small. When joint loading occurs, this may lead to large peak loads, which may cause damage to the cartilage layers on the articular surfaces. The presence of a fibro-cartilaginous disc in the joint is believed to prevent the extreme variations in the loading, since the disc is capable of deforming and adapting its shape to that of the articular surfaces. The magnitude of the deformation and resulting stress of the disc is influenced by the nature of the applied loads and by the biomechanical properties of the disk, such as stiffness and strength.

The mean and standard deviation values (MP) for the tensile strength are summarized in figure 5, whereas compressive strength (MP) and elastic modulus (MP) are summarized in table 2.

Bone contains 85% calcium phosphate, hence ceramics such as hydroxyapatite (HA), tricalcium phosphate and composites such as biphasic calcium phosphate (BCP), have been widely investigated for bone scaffolds [43].

The proposed molecular mechanism for the potentials favorable interaction between chitosan: hydroxyapatite and nano-diamond is based on the unique properties of the materials. In particular, the intermolecular hydrogen bond and chelate interaction between the chitosan and hydroxyapatite promotes favorable mechanical properties [43]. There is a possible interaction between the NH_2 group and primary and secondary -OH group of chitosan with Ca^{2+} (metal coordination interaction) of HAp. This interaction might be responsible for the higher mechanical strength of the composite scaffolds as compared to chitosan and hydroxyapatite alone [43]. Water content of the scaffold may also have a major role to play in the mechanical strength.

Biodegradation

The total weight changes of the hydrogels after dissolving in a phosphate buffered saline (PBS) solution 37°C at pH 7.4 for a period up to 7 days are summarized in figure 6. For all hydrogels containing hydroxyapatite, the weight steadily decreased with incubation time.

Microbiology and hydroxyapatite/nanodiamond hydrogels: *in vitro* investigation

All the test samples gave an average inhibition zone larger than the tetracycline control disc, thereby confirming the antibacterial

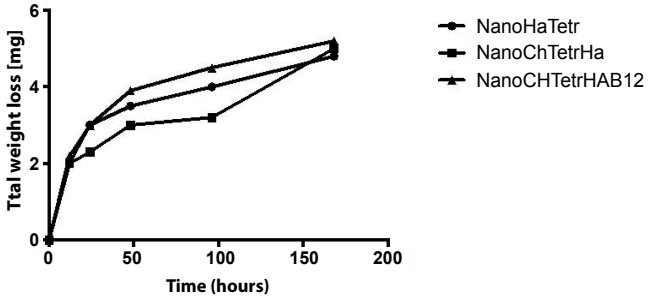

Figure 6: Weight losses of the hydrogels containing HA after dissolution test in a PBS solution at 37°C for periods up to 7 days.

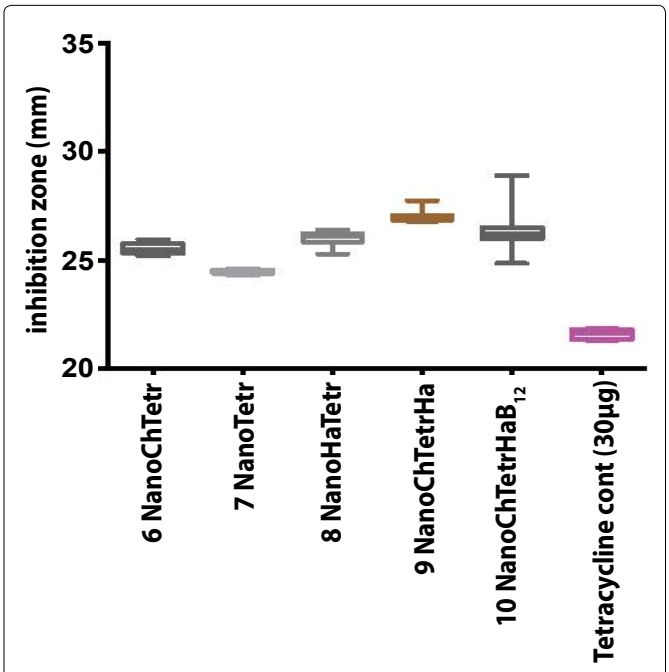

Figure 7: Inhibition Zone against *Staphylococcus aureous*.

activity of the different nano-diamond combinations against *Staphylococcus aureous* (Figure 7) [44]. Using the Student's T-test ($p < 0.01$), there was a significant difference between the rest of the samples when compared to each other and the positive control. The hydrogel with the highest antibacterial activity contained bioactive and hydroxyapatite/chitosan and the antibacterial activity was still higher than the tetracycline control disc (Figure 7).

The process of inflammation plays a crucial role in wound healing. In the event of an injury, inflammatory cells such as the granulocytes, monocytes, and macrophages migrate to the injury site. Fibroblasts are activated by the growth factor that is released, and they produce matrix and new collagen fibrils [39]. But these collagen fibrils do not align with the original connective tissue. Instead, they grow at right angles to the plane of the injury. The integrity of the zone of healing is further compromised as the elastin fibers do not heal at all. Anti-inflammatory medications usually prescribed after injury allay pain and swelling but unfortunately they diminish the healing response [40]. As a result of this incomplete healing, the joint remains painful with normal or even sub normal physical activity. Such a joint may become hypermobile and prone to re-injury due to incomplete ligament support. Newly designed hydrogels may also be beneficial in TMD management owing to its anti-microbial effect. Chlamydia, Mycoplasma genitalium, Staphylococcus aureus, Mycoplasma fermentans, Actinobacillus actinomycetemcomitans, and Streptococcus mitis have been cultured from the TMJ. The presence of *S. aureus* in the TMJ synovial fluid has been related to TMD [44].

Conclusion

In this investigation we prepared several chitosan containing hydrogels with build in nano-diamond and hydroxyapatite and the mechanical properties of the materials was greatly improved based on the classes of bioactive materials, which have proven to be suitability and flexibility of the designer materials to act as an "*in vitro*" probe to gain insights into molecular origin of TMJ. The microbiological evaluation of the new materials was evaluated and activity against *Staphylococcus aureous* was noted in all materials. The drug (such as tetracycline) was released in the sustainable manner. The bioadhesion of the new materials to the dentine as an example of the effective hydroxyapatite model was also assessed.

References

1. Di Silvio L, Bonfield W (1999) Biodegradable drug delivery system for the treatment of bone infection and repair. J Mater Sci Mater Med 10: 653-658.
2. Shinto Y, Uchida A, Korkusuz F, Araki N, Ono K (1992) Calcium hydroxyapatite ceramic used as a delivery system for antibiotics. J Bone Joint Surg Br 74: 600-604.
3. Gittens SA, Uludag H (2001) Growth factor delivery for bone tissue engineering. J Drug Target 9: 407-429.
4. Tabata Y (2000) Necessity of drug delivery systems to tissue engineer ing. In: Park KD (ed) Biomaterials and drug delivery toward the new millennium. Seoul: Han Rim Won Publisher 531-534.
5. Laskin DM (1998) Putting order into temporomandibular disorders. J Oral Maxillofac Surg 56: 121.
6. Laskin DM (1995) Diagnosis and etiology of myofascial pain and dysfunction. Oral Maxillofac Surg Clin North Am 7: 73-78.
7. Dworkin SF, LeResche L (1992) Research diagnostic criteria for temporomandibular disorders: review, criteria, examinations and specifications, critique. J Craniomandib Disord 6: 301-355.
8. Ogle OE, Hertz MB (2000) Myofascial pain. Oral Maxillofac Surg Clin North Am 12: 217-231.
9. Okeson JP (1985) Fundamentals of Occlusion and Temporo-mandibular Disorders. St. Louis: C.V. Mosby.
10. Stohler CS (2000) Masticatory myalgias. In: Fonseca RJ (ed) Oral and Maxillofacial Surgery. Temporomandibular Disorders, Philadelphia: WB Saunders 38-45.
11. Milam SB (2000) Pathophysiology of articular disk displace-ments of the temporomandibular joint. In: Fonseca RJ (ed) Oral and Maxillofacial Surgery. Temporomandibular Disorders, Philadelphia: WB Saunders 46-72.
12. Oliveira JM, Rodrigues MT, Silva SS, Malafaya PB, Gomes ME, et al. (2006) Novel hydroxyapatite/chitosan bilayered scaffold for osteochondral tissue-engineering applications: Scaffold design and its performance when seeded with goat bone marrow stromal cells. Biomaterials 27: 6123-6137.
13. Westesson PL, Eriksson L, Kurita K (1989) Reliability of a negative clinical temporomandibular joint examination: prevalence of disk displacement in asymptomatic temporo-mandibular joints. Oral Surg Oral Med Oral Pathol 68: 551-554.
14. Boccaccini AR, Blaker JJ, Maquet V, Day RM, Jérôme R (2005) Preparation and characterisation of poly(latide-co-glycolide) (PLGA) and PLGA/Bioglass Composite Tubular Foam Scaffolds for Tissue Engineering Applications. Mater Sci & Eng C 25: 23-31.
15. Perchyonok VT, Grobler SR, Zhang S (2014) IPNs from Cyclodextrin:Chitosan Antioxidants: Bonding, Bio-Adhesion, Antioxidant Capacity and Drug Release. J Funct Biomater 5: 183-196.
16. Perchyonok VT, Reher V, Basson NJ, Zhang S, Grobler SR (215) Bioinspired-Interpenetrating Network (IPNs) Hydrogel (BIOF-INPs) and TMD in Vitro: Bioadhesion, Drug Release and Build in Free Radical Detection and Defense, Open Journal of Stomatology 5: 53-61.
17. Perchyonok VT, Reher V, Grobler SR, Oliver A, Zhang S (2015) Bioactive-Functionalized Interpenetrating Network Hydrogel (BIOF-IPN): A Novel Biomaterial Transforming the Mechanism of Bio-Repair, Bio-Adhesion and Therapeutic Capability – An *In Vitro* Study. J Interdiscipl Med Dent Sci 3: 166.
18. Vinklárková L, Masteiková R, Vetchý D, Doležel P, Bernatonienė J (2015) Formulation of Novel Layered Sodium Carboxymethylcellulose Film Wound Dressings with Ibuprofen for Alleviating Wound Pain. Biomed Res Int 2015: 892671.
19. Souza RM, de Souza MC, Patitucci ML, Silva JF (2007) Evaluation of antioxidant and antimicrobial activities and characterization of bioactive components of two Brazilian propolis samples using a pKa-guided fractionation. Z Naturforsch C 62: 801-807.
20. Hung CF, Lin YK, Huang ZR, Fang JY (2008) Delivery of resveratrol, a red wine polyphenol, from solutions and hydrogels via the skin. Biol Pharm Bull 31: 955-962.
21. Singh B, Pal L (2012) Sterculia crosslinked PVA and PVA-poly(AAm) hydrogel wound dressings for slow drug delivery: mechanical, mucoadhesive, biocompatible and permeability properties. J Mech Behav Biomed Mater 9: 9-21.
22. Zeighampour F, Sichani MM, Shams E, Naghavi NS (2014) Antibacterial Activity of Propolis Ethanol Extract against Antibiotic Resistance Bacteria Isolated from Burn Wound Infections. J Res Med Sci 16: 25-30.
23. Mirzoeva OK, Grishanin RN, Calder PC (1997) Antimicrobial action of propolis and some of its components: the effects on growth, membrane potential and motility of bacteria. Microbiol Res 152: 239-246.
24. Wojtyczka RD1, Kępa M, Idzik D, Kubina R, Kabała-Dzik A, et al. (2013) In Vitro Antimicrobial Activity of Ethanolic Extract of Polish Propolis against Biofilm Forming Staphylococcus epidermidis Strains. Evid Based Complement Alternat Med 2013: 590703.
25. Berretta AA, de Castro PA, Cavalheiro AH, Fortes VS, Bom VP, et al. (2013) Evaluation of Mucoadhesive Gels with Propolis (EPP-AF) in Preclinical Treatment of Candidiasis Vulvovaginal Infection. Evid Based Complement Alternat Med 2013: 641480.
26. Mirzoeva OK, Grishanin RN, Calder PC (1997) Antimicrobial action of propolis and some of its components: the effects on growth, membrane potential and motility of bacteria. Microbiol Res 152: 239-246.
27. Bauer AW, Kirby WM, Sherris JC, Turck M (1966) Antibiotic susceptibility testing by a standardized single disk method. Am J Clin Pathol 45: 493-496.
28. Kalpakci KN, Willard VP, Wong ME, Athanasiou KA (2011) An interspecies comparison of the temporomandibular joint disc. J Dent Res 90: 193-198.
29. Jones KE, Ruff CB, Goswami A (2013) Morphology and biomechanics of the pinniped jaw: mandibular evolution without mastication. Anat Rec (Hoboken) 296: 1049-1063.
30. BAUER AW, PERRY DM, KIRBY WM (1959) Single-disk antibiotic-sensitivity testing of staphylococci; an analysis of technique and results. AMA Arch Intern Med 104: 208-216.
31. Bauer AW, Kirby WM, Sherris JC, Turck M (1966) Antibiotic susceptibility testing by a standardized single disk method. Am J Clin Pathol 45: 493-496.
32. Ananth AN, Daniel SC, Sironmani TA, Umapathi S (2011) PVA and BSA stabilized silver nanoparticles based surface-enhanced plasmon resonance probes for protein detection. Colloids Surf B Biointerfaces 85: 138-144.
33. Borges JG, Tagliamento M, Silva AG, do Amaral Sobral PJ, de Carvalho RA (2013) Development and characterization of orally-disintegrating films for propolis delivery. Cienc Tecnol Aliment 33: 28.
34. Barud Hda S, de Araújo Júnior AM, Saska S, Mestieri LB, Campos JA, et al. (2013) Antimicrobial Brazilian Propolis (EPP-AF) Containing Biocellulose Membranes as Promising Biomaterial for Skin Wound Healing. Evid Based Complement Alternat Med 2013: 703024.
35. de Almeida BM, do Nascimento MF, Pereira-Filho RN, de Melo GC, dos Santos JC , et al. (2014) Immunohistochemical profile of stromal constituents and lymphoid cells over the course of wound healing in murine model. Acta Cir Bras.
36. Chastain SR, Kundu AK, Dhar S, Calvert JW, Putnam AJ (2006) Adhesion of mesenchymal stem cells to polymer scaffolds occurs via distinct ECM ligands and controls their osteogenic differentiation. J Biomed Mater Res A 78: 73-85.
37. Arzi B, Winer JN, Kass PH, Verstraete FJ (2013) Osteoarthritis of the temporomandibular joint in southern sea otters (Enhydra lutris nereis). J Comp Pathol 149: 486-494.
38. Arzi B1, Cissell DD, Verstraete FJ, Kass PH, DuRaine GD, et al. (2013) Computed tomographic findings in dogs and cats with temporomandibular joint disorders: 58 cases (2006-2011). J Am Vet Med Assoc 242: 69-75.
39. Henry CH, Hughes CV, Gérard HC, Hudson AP, Wolford LM (2000) Reactive arthritis: preliminary microbiologic analysis of the human temporomandibular joint. J Oral Maxillofac Surg 58: 1137-1142.
40. Tanaka E, del Pozo R, Tanaka M, Asai D, Hirose M, et al. (2004) Three-dimensional finite element analysis of human temporomandibular joint with and without disc displacement during jaw opening. Med Eng Phys 26: 503-511.
41. Woodard JR, Hilldore AJ, Lan SK, Park CJ, Morgan AW, et al. (2007) The mechanical properties and osteoconductivity of hydroxyapatite bone scaffolds with multi-scale porosity. Biomaterials 28: 45-54.
42. Kim HW, Lee SY, Bae CJ, Noh YJ, Kim HE, et al. (2003) Porous ZrO_2 bone scaffold coated with hydroxyapatite with fluorapatite intermediate layer. Biomaterials 24: 3277-3284.
43. Miao X, Tan LP, Tan LS, Huang X (2007) Porous calcium phosphate ceramics modified with PLGA bioactive glass. Mater Sci & Eng C 27: 274-279.
44. Bauer AW, Kirby WM, Sherris JC, Turck M (1966) Antibiotic susceptibility testing by a standardized single disk method. Am J Clin Pathol 45: 493-496.